3-22-2021

Feasibility of using a high-power electromagnetic energy harvester to power structural health monitoring sensors and systems in transportation infrastructures

Mohsen Amjadian
The University of Texas Rio Grande Valley, mohsen.amjadian@utrgv.edu

Anil K. Agrawal

Hani Nassif

Recommended Citation

Amjadian, Mohsen, Anil K. Agrawal, and Hani Nassif. "Feasibility of using a high-power electromagnetic energy harvester to power structural health monitoring sensors and systems in transportation infrastructures." In Sensors and Smart Structures Technologies for Civil, Mechanical, and Aerospace Systems 2021, vol. 11591, pp. 285-294. SPIE, 2021. https://doi.org/10.1117/12.2585257

Feasibility of using a high-power electromagnetic energy harvester to power structural health monitoring sensors and systems in transportation infrastructures

Mohsen Amjadian*[a] Anil. K. Agrawal [a], and Hani Nasif [b]

[a] Department of Civil Engineering, The City University of New York (City College), 160 Convent Ave., New York, NY 10031.

[b] Department of Civil and Environmental Engineering, Rutgers University-New Brunswick, 500 Bartholomew Road Piscataway, NJ 08854.

ABSTRACT

This paper investigates the feasibility of an electromagnetism energy harvester (EMEH) for scavenging electric energy from transportation infrastructures and powering of conventional sensors used for their structural health monitoring. The proposed EMEH consists of two stationary layers of three cuboidal permanent magnets (PMs), a rectangular thick air-core copper coil (COIL) attached to the free end of a flexible cantilever beam whose fixed end is firmly attached to the highway bridge oscillating in the vertical motion due to passing traffic. The proposed EMEH utilizes the concept of creating an alternating array of permanent magnets to achieve strong and focused magnetic field in a particular orientation. When the COIL is attached to the cantilever beam and is placed close to the PMs, ambient and traffic induced vibration of the cantilever beam induces eddy current in the COIL. The tip mass and stiffness of the cantilever beam are adjusted such that a low-frequency vibration due to the passing traffic can effectively induce the vibration of the cantilever beam. This vibration is further amplified by tuning the frequency of the cantilever beam and its tip mass to resonance frequency of the highway bridge. The numerical results show that the proposed EMEH is capable of producing an average electrical power more than 1 W at the resonance frequency 4 Hz over a time period of 1 second that alone is more than enough to power conventional wireless sensors.

Keywords: Highway bridge, sensor, energy harvesting, permanent magnet, copper coil, resonance, electrical power.

1. INTRODUCTION

Fossil fuels such as coal and petroleum are the primary sources of energy. They are, however, nonrenewable, and more importantly harmful to our health and environment when being converted to motion energy. A large portion of fossil fuel-derived energy is consumed by vehicles moving daily in urban areas which is one of the major sources of air pollutants. The motion of vehicles is, however, a significant source of kinetic energy that can be harvested to power sensors and electrical equipment installed on highway bridges for structural health monitoring, thereby reducing some dependence on fossil fuel-derived energy. This reduces the cost of structural health monitoring by eliminating wiring requirements for an external power outlet [1,2].

There are three different types of energy harvesters typically used to harvest electric power from traffic induced-vibration which are: electromagnetic, piezoelectric, and electrostatic [1,3]. Electromagnetic energy harvesters (EMEHs) are more reliable among them because they do not require mechanical contact between any components. For this reason the effects of wear and tear is minimal in EMEHs, which can reduce the unwanted mechanical damping in the harvester. The basic mechanism of an EMEH is based on the Faraday's law of induction [4,5]. The relative motion between a permanent magnet (PM) and a conductive medium (e.g. copper coil) causes a change in the magnetic flux of the PM passing through the conductive medium. This change induces the so-called eddy current inside the conductive medium and the direction of this electric current opposes the change in the external magnetic flux because of the relative motion of the PM and the conductive medium as per the Lenz's law [6–8].

A large number of studies have focused on small sized EMEHs with single-frequency resonance which are referred to as narrow-band EMEHs. In these energy harvesters, the fundamental mode of vibration is usually tuned to resonate with the

* Post-doctoral Fellow; Email: mamjadian@ccny.cuny.edu; Phone: +1 212-650-8067; Fax: +1 212-650-6965.

first significant frequency of the external excitation. The optimization of these types of EMEHs is limited to the components of the harvesting circuit [9–17]. In the recent decade, a specific attention has been devoted to wide-band EMEHs in which the first several significant modes of vibration of the EMEH are tuned to resonate with the first several significant frequencies of the external excitation. Some examples are piecewise-linear harvester [18], multi-frequency harvester with FR4 coils (Yang et al., 2009), locally resonant harvester [19], and multi-frequency harvester with magnetic spring [20]. The design of these types of EMEHs is complicated, and they are expensive to implement.

A scaling study has shown that, contrary to what commonly believed, the power density of an EMEH does not decrease proportionately with its volume as far as the electromechanical coupling remain strong [21]. One of the effective methods to strengthen the electromechanical coupling in an EMEH is to optimize the arrangement of permanent magnets (PMs) poles in order to strengthen their magnetic field toward the copper coil. This paper focuses on the numerical simulation of a high-power EMEH consisting of PMs with linear pole arrangements. The objective of the study is to optimize the design of the EMEH such that it will be able to generate an average power of 1W and higher. This amount of electrical energy is sufficient to power conventional sensors installed on highway bridges with low-frequency vibrations [17,22].

2. MATHEMATICAL MODELING

Figure 1 shows the configuration of the EMEH consisting of a rectangular thick air-core copper coil (COIL) moving relative to two layers of three cuboidal permanent magnets (PMs) mounted on the left and right sides of the COIL. These PMs are attached to a firm base linked to the bridge that moves with the acceleration $\ddot{u}_{bX}(t)$ along the X-axis. The COIL is attached to this base through a thin flexible cantilever beam. The size of the horizontal air gap between the COIL and the left and right layers of PMs along the Z-axis is denoted by Δ_{gZ}, and the size of the air gap between the PMs along the X-axis is denoted by δ_{gX}.

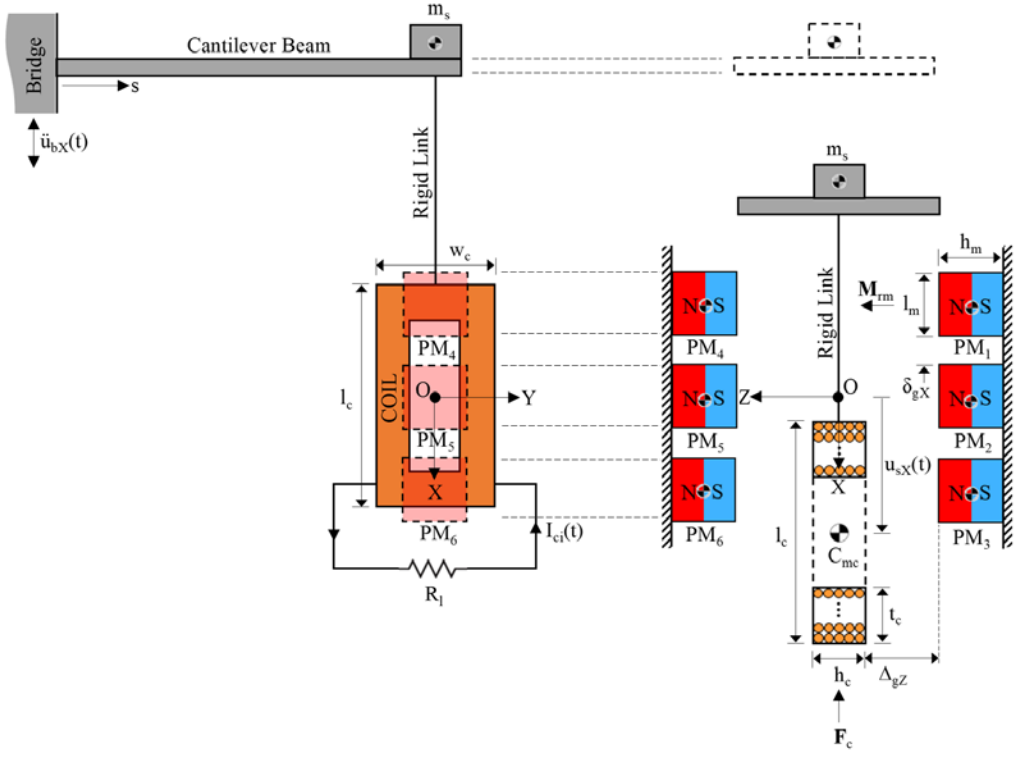

Figure 1. Configuration of the EMEH consisting of a cantilever beam, a rectangular thick air-core copper coil and two layers of three cuboidal permanent magnets.

The PMs are identical and each has the dimensions $l_m \times w_m \times h_m$. The dimensions of the left and right layers of PMs are then calculated to be $L_m=3l_m+2\delta_{gmX}$, $W_m=w_m$, and $H_m=h_m$. The COIL, as shown in Figure 1, has the dimensions $l_c \times w_c \times h_c$, the winding depth t_c, and the total number of turns $N_c=N_Z \times N_t$, where N_Z and N_t are the numbers of turns

along the Z-axis and the depth of the winding, respectively. It is ideally assumed that $N_Z=h_c/d_w$ and $N_t=t_c/d_w$ where d_w is the diameter of the winding wire made of copper. It is assumed that $I_{ci}(t)>0$ when the electric current $I_{ci}(t)$ is counterclockwise in the XY-plane so that the N- and S-poles are established at $Z=+h_c/2$ and $Z=-h_c/2$, respectively, otherwise $I_{ci}(t)<0$.

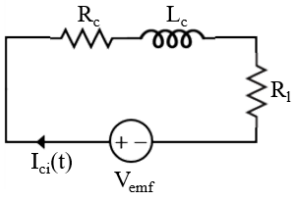

Figure 2. RL circuit model of the EMEH including an electric load with the resistance R_l.

A RL circuit consisting of a resistor with the resistance R_l (electrical load) connected to the COIL in series is used to harvest the electric power P_l from the EMEH as shown in Figure 2. Here, the COIL is represented by a resistor with the resistance R_c in series with an inductor with the induction L_c whose values are functions of the COIL's geometry. The electric power is generated by the electromagnetic induction occurring in the COIL when it moves relative to the PMs. This relative motion causes a change in the magnetic flux of the PMs passing through the COIL which induces the electromotive force V_{emf} in the circuit as per the Faraday's law of induction, and as a result, the electric current $I_{ci}(t)$ is flowed through the COIL. It should be noted that the direction of this electric current changes as per the Lenz's law in such a way that the magnetic field of the COIL opposes the initial cause of change in the magnetic flux of the PMs which is the motion of the COIL. This magnetic interaction eventually excretes the magnetic force $\mathbf{F}_c$ on the COIL opposing to its motion, acting as a nonlinear braking/damping force.

2.1 Electromechanical equation

The motion of the COIL through the magnetic field of the PM_S when the beam is subjected to the base acceleration $\ddot{u}_{bX}(t)$ is described by the following coupled equations representing the electromechanical behavior of the system:

$$m_b \frac{\partial^2 w_{bX}(s,t)}{\partial t^2} + c_b \frac{\partial w_{bX}(s,t)}{\partial t} + E_b I_b \frac{\partial^4 w_{bX}(s,t)}{\partial s^4} = -m_b \ddot{u}_{bX}(t) \tag{1a}$$

$$L_c \frac{dI_{ci}(t)}{dt} + \left(R_l + R_c\right) I_{ci}(t) = V_{emf}(t) \tag{1b}$$

where, in Equation (1a), m_b and c_b are the mass and mechanical damping per unit length of the beam, respectively, E_bI_b is the flexural rigidity of the beam, and $w_b(s,t)$ is the transverse displacement of the beam along the X-axis relative to the base. The free end of the beam is subjected to force F_{cX} which is the X-component of the magnetic force $\mathbf{F}_c$ excreted on the COIL attached to the beam at s=L. This force and the tip (proof) mass m_s representing the mass of the COIL and its associated components are taken into account by satisfying the force boundary condition at s=L [23–25]. The tip mass can be increased to tune the fundamental frequency of the beam to the excitation frequency, thereby increasing the amplitude of the vibration and the output electrical power.

2.2 Magnetic force

The magnetic force $\mathbf{F}_c$ is given by,

$$\mathbf{F}_c = \sum_{I=1}^{3} \left(\mathbf{F}_{cI}\right)_{RL} + \sum_{I=4}^{6} \left(\mathbf{F}_{cI}\right)_{LL} \tag{2a}$$

where $\mathbf{F}_{cI}$ is the magnetic force excreted on the COIL when it is subjected to magnetic field of the I-th PM in the left and right layers of the PMs. This force can be calculated by the Lorentz force for current-carrying wires as follows [26],

$$\mathbf{F}_{cI} = I_{ci} \oint_{wire} d\mathbf{l} \times \mathbf{B}_I \tag{2b}$$

This is a line integral taken over the length of the copper wire in which $\mathbf{B}_I$ is the magnetic flux density vector of I-th PM with the magnetization vector $\mathbf{M}_{rmI}=+M_{rmI}\mathbf{e}_Z$ that is given by [27,28],

$$\mathbf{B}_I(X,Y,Z) = -\frac{1}{4\pi} B_{rmI} \sum_{i,j,k=1}^{2} (-1)^{i+j+k} \begin{Bmatrix} b_X(X-X_{cIi}, Y-Y_{cIj}, Z-Z_{cIk}) \\ b_Y(X-X_{cIi}, Y-Y_{cIj}, Z-Z_{cIk}) \\ b_Z(X-X_{cIi}, Y-Y_{cIj}, Z-Z_{cIk}) \end{Bmatrix} \tag{3a}$$

where $X=X_{cI1}$, $X=X_{cI2}$, $Y=Y_{cI1}$, $Y=Y_{cI2}$, $Z=Z_{cI1}$, and $Z=Z_{cI2}$ are the coordinates of the boundary surfaces surrounding the volume of the I-th PM with respect to the X-, Y-, and Z-axes, respectively, B_{rmI} is the magnetic remanence of the I-th PM defined as $B_{rmI}=\mu_0 M_{rmI}$ in which $\mu_0=4\pi\times10-7$ Tm/A is the magnetic permeability of the vacuum, and functions b_X, b_Y, and b_Z are defined as follows,

$$b_X = \ln(Y+R) \quad , \quad b_Y = \ln(X+R) \quad , \quad b_Z = \tan^{-1}(YZ/XR) + \tan^{-1}(XZ/YR) \tag{3b}$$

where $R=(X^2+Y^2+Z^2)^{1/2}$. It is a tedious task to calculate force $\mathbf{F}_{cI}$ using the integral described by Equation (2b) because the integral is involved and numerically difficult to compute. A more efficient way is to approximate each turn of the COIL with an equivalent PM with the magnetization vector $M'_{rm}=+(N_z I_{ci}/h_c)\mathbf{e}_Z$ and then calculate force $\mathbf{F}_{cI}$ by summing up the magnetic forces between the PMs and each turn of the COIL as described in the previous works of the author [29–31].

2.3 Induced voltage

The electromotive force V_{emf} is given by,

$$V_{emf} = \sum_{I=1}^{3} (V_{emfI})_{RL} + \sum_{I=4}^{6} (V_{emfI})_{LL} \tag{4a}$$

where V_{emfI} is the electromotive force (EMF) induced in the COIL when it is subjected to magnetic field of the I-th PM located in the left and right layers of the PMs, which can be calculated by the following formula [26],

$$V_{emfI} = \int_{wire} (\mathbf{v}_c \times \mathbf{B}_I) \bullet d\mathbf{l} \tag{4b}$$

where $\mathbf{v}_c=+\dot{u}_{sX}\mathbf{e}_X$ is the velocity vector of the COIL moving along the X-axis. This line integration is taken over the length of the copper wire in which $\mathbf{B}_I$ is given by Equation (3).

2.4 Electromechanical coupling coefficient

Equation (2b) can be rewritten into the following form

$$F_{cX} = -K_f I_{ci} \tag{5}$$

where K_f is called electromechanical coupling coefficient or transformation factor [9] that couples the mechanical domain to the electrical domain. This coefficient is time varying because the limits of integration in Equation (2a) changes with the motion of the COIL. However, a quite large number of researchers [2,10,32–34] have assumed that K_f is constant and does not change with time which is an oversimplified assumption that may lead to error in estimation of the harvested electric power [35,36]. It can be also shown that,

$$V_{emf} = +K_f \dot{u}_{sX} \tag{6}$$

Equations (5) and (6) show that how the generation of the electromotive force V_{emf} (and the alternating current $I_{ci}=V_{emf}/(R_l+R_c)$) in the RL circuit is coupled to the velocity of the COIL and its magnetic interaction with the PMs.

2.5 SDOF model

It is more convenient to approximate the response of the cantilever beam with its response in the first mode of vibration which is in resonance with the external excitation. This approximation becomes more accurate when the tip mass is much larger than the total mass of the beam [25,37]. If we assume that $m_s/m_bL\rightarrow\infty$ then the governing equation can be written into the following form by eliminating $I_{ci}(t)$ from Equation (1) using Equations (5) and (6),

$$\ddot{u}_{sX}(t)+2\left(\xi_s+\frac{K_f^2(t)}{2m_s\omega_s\left(R_l+R_c\right)}\right)\omega_s\dot{u}_{sX}(t)+\omega_s^2u_{sX}(t)=\ddot{u}_{bX}(t) \tag{7}$$

where $\omega_s=2\pi f_s$ is the natural circular frequency of the first mode of the beam in which f_s being the natural frequency, ξ_s is the critical mechanical damping ratio, and $u_{sX}(t)$ is the displacement of the free end of the beam or the COIL along the X-axis. This equation is nonlinear due to time variant nature of the electromechanical coupling coefficient $K_f(t)$. A numerical solver is used in SIMULINK [38] to solve it. The electrical power harvested from the EMEH is equal to the instantaneous power P_l consumed by the load which is given by,

$$P_l(t)=R_lI_{ci}^2(t) \tag{8a}$$

The parameter used to assess the performance of the EMEH is the average electrical power P_{lavg} given by the following integral taken over time interval $[0,\tau]$,

$$P_{lavg}=\frac{1}{\tau}\int_0^{\tau}P_l(t)dt \tag{8b}$$

3. PARAMETRIC STUDY

A parametric study is carried out in this section to optimize the configuration of the EMEH and its performance in harvesting electrical power from the traffic-induced vibration of highway bridges. The excitation of the base is assumed to be harmonic with the acceleration $\ddot{u}_{bX}(t)=\ddot{u}_{bXmax}\sin(2\pi f_bt)$ in which $\ddot{u}_{bXmax}$ and f_b are the amplitude and frequency, respectively. These parameters are set to $\ddot{u}_{bXmax}=0.1g$ and $f_b=4$ Hz which are common values for highway bridges subjected to traffic loading [17]. The response of the EMEH is a function of these parameters Δ_{gZ}, δ_{gX}, l_c, w_c, h_c, t_c, d_w, l_m, w_m, h_m, B_{rm}, m_s, f_s, ξ_s, R_c, R_l, and τ. In this study, it is assumed that the PMs are cubic shaped with the size $l_m=w_m=h_m=a_m=1$ in and $B_{rm}=1.4$ T. It is further assumed that $\Delta_{gZ}=1/16$ in, $d_w=1$ mm (18-AWG), $R_c=2.173\ \Omega$ (for l_w=copper wire length=100 ft), $m_s=704$ gr (mass of the copper wire), $f_s=4$ Hz, $\xi_s=0.05$, and $\tau=1$ sec. The rest of parameters including the dimensions of the COIL, δ_{gX}, and R_l referred to as optimization parameters (OPTPs) are varied to optimize the performance of the EMEH.

3.1 Dimensions of the COIL

The COIL is assumed to be cuboidal shaped with the length l_c, the width w_c, the height h_c, and the winding depth t_c. The length of the copper wire l_w winding the COIL is kept as a constant here that can be expressed in terms of the dimensions of the COIL as $l_w=2N_zN_t(l_c+w_c-2t_c)$. This expression is used to set up to following formula to find h_c in term of l_w, N_t, and d_w,

$$h_c=\frac{l_w}{2N_t^2\left[\left(1+\alpha_c\right)\left(\frac{l_c}{N_td_w}\right)-2\right]} \tag{9}$$

where $\alpha_c=w_c/l_c<1$ is the aspect ratio of the COIL on the XY-plane. It should be noted that $N_t<0.5\alpha_c(l_c/d_w)$ to make sure that the winding depth t_c remains less than the half of the width in accordance with the physics of the problem. The length of the COIL is fixed to be same as the length of the left and right PMs layers. This ensures that a minimal motion can cause the COIL to cut through the magnetic field of the PMs at the edges where the magnetic flux density varies sharply. The rest of OPTPs are assumed to have these values: $\delta_{gX}=1$ mm and $R_l=R_c=2.173\ \Omega$.

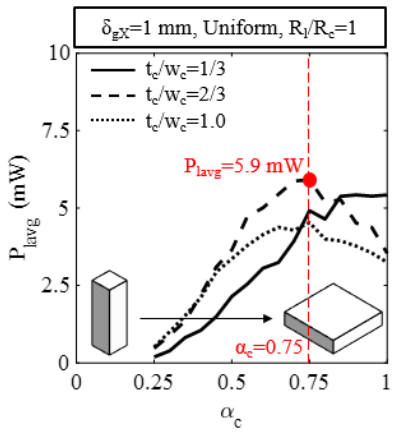

Figure 3. Effects of the geometry of the COIL on the harvested electrical power.

Figure 3 shows the variation of P_{lavg} with α_c for three different values of the winding depth: t_c/w_c=1/3, 2/3, and 3/3. It is seen that P_{lavg} increases with the increase of α_c implying that the more flatter the COIL, the higher electrical power can be harvested. The maximum harvested electrical power is equal to 5.9 mW that is obtained when α_c=0.75 and t_c/w_c=2/3 as illustrated in this figure. Therefore, the optimum dimensions of the COIL are l_c=3.079 in, w_c=2.309 in, h_c=1.048 in, and t_c=0.761 in.

3.2 Arrangement of the PMs

The arrangement of the PMs based on the direction of their poles and the size of the air gap between them can significantly affect their magnetic interaction with the COIL. Figure 2 shows two different arrangements of the PMs poles considered for evaluation of the EMEH in this study: (a) uniform and (b) alternating linear arrays. Figure 4(a) and (b) show the variation of P_{lavg} with δ_{gmX} when the PMs are arranged according to the uniform and alternating linear arrays, respectively. The optimum dimensions of the COIL found in sub-section 3.1 have been used here with this assumption that $R_l=R_c$=2.173 Ω. Figure 4(a) shows that the variation of P_{lavg} with δ_{gmX} is harmonic-like for the uniform linear array, i.e. $P_{lavg}\sim-\sin(\delta_{gmX})$. It first decreases and then increases as the thickness of the air gap between the PMs becomes larger. The maximum harvested electrical power is equal to 8.068 mW that is generated when δ_{gmX}=0.75 in (red circle). Figure 4(b), however, shows that the variation of P_{lavg} with δ_{gmX} is bell-like for the alternating linear array. The maximum electrical power is calculated to be 269.4 mW which is remarkably larger than that calculated for the uniform linear array. This peak also happens when δ_{gmX}=3/4 in (red circle). It is seen that at very large gaps $\delta_{gmX}>a_m$=1 in (black circle) the performances of both the linear arrays become similar as expected which is due to the fact that the magnetic interaction of the COIL with each PMs become independent from its magnetic interaction with other PMs. Therefore, the alternating linear array causes the highest amount of electrical power that can be harvested from the EMEH.

3.3 Electrical load

The electrical resistance of the harvesting circuit (electrical load) R_l can also significantly affect the performance of the EMEH and the amount of electrical power that can be extracted from it. This is a key parameter that can help to configure the electrical components of the harvesting circuit and its resultant resistance. Figure 5(a) shows the variation of P_{lavg} with R_l/R_c for the case when the PMs are arranged according to the alternating linear array with this assumption that δ_{gmX}=3/4 in. The optimum dimensions of the COIL found in sub-section 3.1 have been used here. It is seen that the maximum harvested electrical power is equal to 1716 mW that is obtained for $R_l=0.25R_c$=0.543 Ω or let say for a circuit with the equivalent electrical resistance of 0.5 Ω. It can also be seen that for $R_l>R_c$ the harvested electrical power decreases dramatically which is due to this valid assumption that the electromechanical coupling coefficient K_f is a time-varying parameter. If we assume that K_f is constant and it does not change with time [2,10,32–34] then the maximum harvested electrical power is obtained when $R_l>R_c$ which is not consistent with the reality of the problem [35,36].

3.4 Base excitation

The dynamic properties of the base acceleration including its amplitude and frequency can have significant effects on the performance of the EMEH. Figure 5(b) shows that to amplify the outputted electrical power it is essential to tune the

fundamental frequency of the EMEH to the excitation frequency. A small decreasing in the peak acceleration of the traffic vibration from 0.1g to 0.075g (i.e., 25%) decreases the maximum electrical power from 1716 mW to 94.65 mW (i.e., 95 %), which is a significant reduction. This shows the importance of identification of the characteristics of the acceleration signal response of the target bridge before finalizing the design of the EMEH.

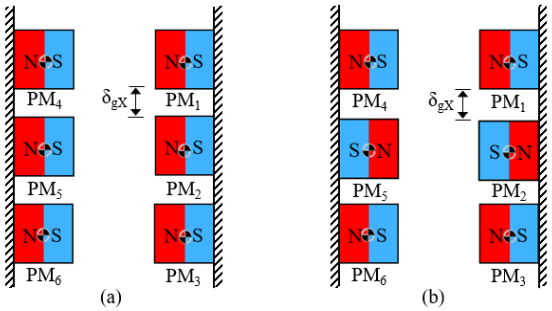

Figure 3. Two different arrangements of the PMs poles proposed for the design of the EMEH: (a) uniform and (b) alternating.

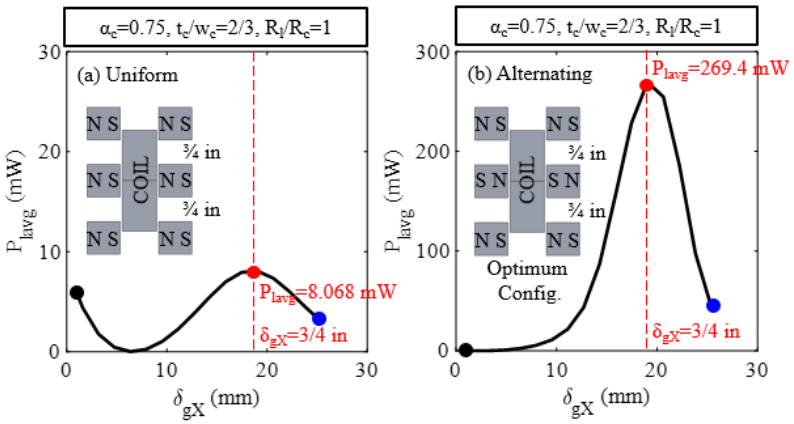

Figure 4. Effects of the arrangement of the PMs on the harvested electrical power: (a) uniform and (b) alternating linear arrays.

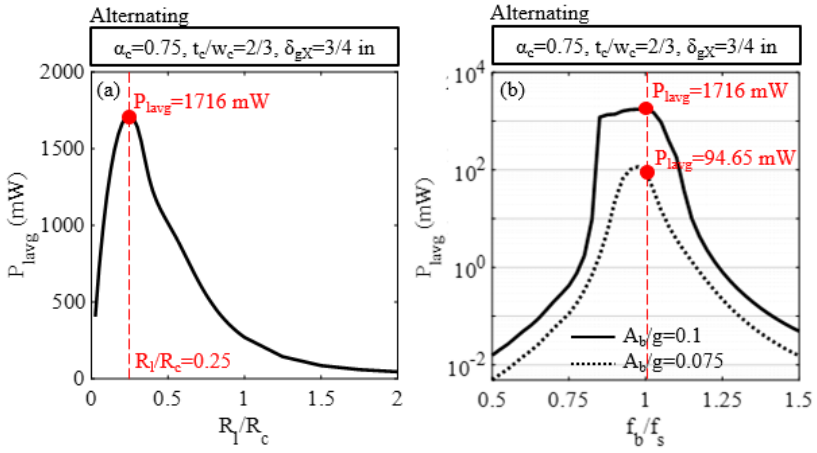

Figure 5. Effects of the (a) electrical resistance of the harvesting circuit and (b) dynamic characteristics of the traffic vibration on the harvested electrical power.

4. NUMERICAL VALIDATION

A three-dimensional finite element (FE) model of the proposed EMEH is developed in COMSOL multiphysics software [39] to verify the accuracy of Equations (2) and (5). The configuration of the FE model has been optimized according to the

results of the parametric analysis performed in section 3. Figures 6(a) shows this model and the details of the meshing. As can be seen a very fine mesh has been used along the edges of the COIL and PMs to achieve accurate results from the simulation. Figure 6(b) shows that the FE model is enclosed by a sphere of the radius r_a=6 in as the air domain whose center is positioned at the origin of the XYZ coordinate system which is located at the center of the air gap between the PMs. Figure 6(c) shows the magnetic flux density vector field of the PMs on the XZ-plane at Y=0 for u_{sX}=−0.322l_c and I_{ci}=−6.2 A.

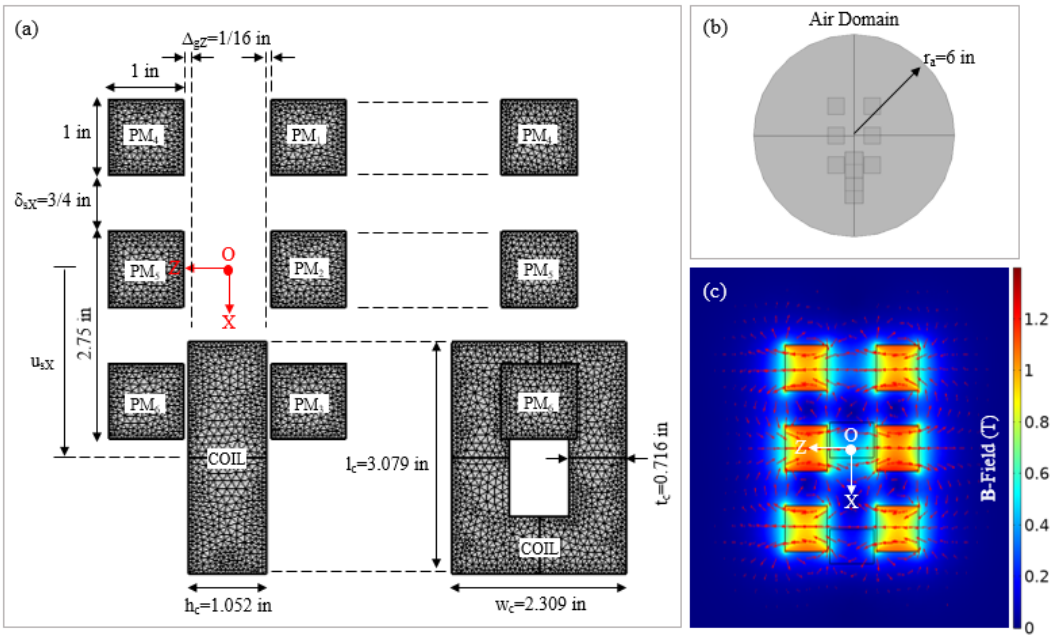

Figure 6. FE model of the EMEH developed in COMSOL: (a) meshing details, (b) air domain, and (c) magnetic flux density vector field of the PMs.

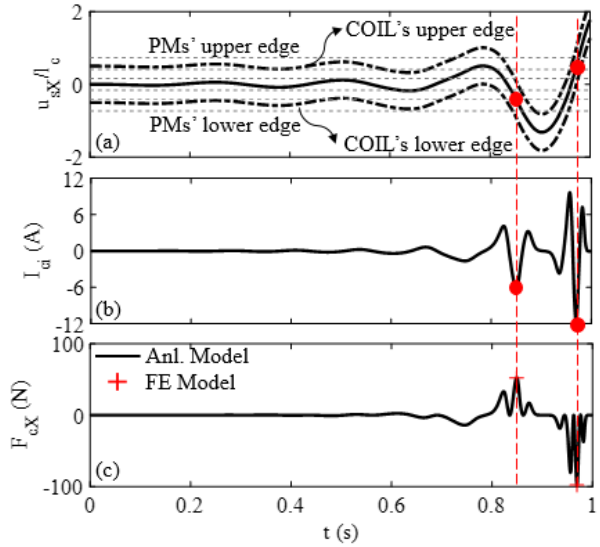

Figure 7. Comparison between the analytical model and the FE model to calculate the magnetic force; (a) displacement of the COIL, (b) electric current induced in the COIL, and (c) magnetic force F_{cX} acting on the COIL.

Figures 7(a) to 7(c) show time histories of the displacement of the COIL u_{sX}, the induced electric current I_{ci}, and the magnetic force acting on the COIL F_{cX}, respectively. This force has been calculated from the analytical model for given

values of u_{sX} and I_{ci} and will be compared to the corresponding results calculated from the FE model. Figures 7(a) and shows two points (red circle) chosen to calculate the magnetic force acting on the COIL where $u_{sX}=-0.322l_c$ and $+0.320l_c$, respectively. These displacements correspond to the electric currents $I_{ci}=-6.2$ A and -11.6 A, respectively, as illustrated on Figure 7(b). Figure 7(c) shows the values of the corresponding magnetic force F_{cX} acting on the COIL calculated from the FE model and then compared to the analytical model. It can be seen that there is a good agreement between both the models at both the points. This validates the accuracy of the analytical model developed to calculate the magnetic force using Equations (2) and (5).

5. CONCLUSIONS

This paper focuses on optimization of the design of high-power narrow band EMEH to be able to generate an average electrical power of about 1 W and more at the resonance frequency 4 Hz. This amount of electrical energy alone is more than enough to power conventional wireless sensors used for their structural health monitoring. The proposed EMEH consists of two stationary layers of three cuboidal PMs, a rectangular thick air-core copper coil (COIL) attached to the free end of a flexible cantilever beam whose fixed end is firmly attached to the highway bridge oscillating in the vertical motion due to passing traffic. An analytical model has been developed to conduct a parametric study and optimize the geometry of the COIL, the arrangement of the PMs, and the resistance of the harvesting circuit. This analytical model has been validated by a FE simulation in COMSOL. It has been shown that arranging the PMs in an alternating layout can significantly increase the generated power if the thickness of the air gap between the PMs to be large enough to amplify the magnetic interaction between the PMs. The numerical results show that the maximum harvested electrical power is equal to 1716 mW obtained by a harvesting circuit with an electrical resistance of 0.5 Ω. It is worth mentioning that the main drawback of the proposed EMEH is its large vibration amplitude that limits its field application. A mechanical stopper can be installed to limit the amplitude of the COIL, although this can to some extent limit the amount of output electrical power [40].

ACKNOWLEDGEMENTS

This research has been funded by the Connected Cities for Smart Mobility towards Accessible and Resilient Transportation (C2SMART) Center, a Tier 1 University Center awarded by U.S. Department of Transportation under the University Transportation Centers Program, which is herewith gratefully acknowledged.

REFERENCES

[1] Roundy, S., Wright, P. K. and Rabaey, J. M., [Energy Scavenging for Wireless Sensor Networks], Springer US (2004).

[2] Williams, C. B. and Yates, R. B., “Analysis of a micro-electric generator for microsystems,” Sensors Actuators, A Phys. **52**(1–3), 8–11 (1996).

[3] Priya, S. and Inman, D. J., [Energy harvesting technologies], Springer US (2009).

[4] Khaligh, A., Zeng, P. and Zheng, C., “Kinetic energy harvesting using piezoelectric and electromagnetic technologiesstate of the art,” IEEE Trans. Ind. Electron. **57**(3), 850–860 (2010).

[5] Wei, C. and Jing, X., “A comprehensive review on vibration energy harvesting: Modelling and realization,” Renew. Sustain. Energy Rev. **74**, 1–18 (2017).

[6] Amjadian, M. and Agrawal, A. K., “Planar Arrangement of Permanent Magnets in Design of a Magneto-Solid Damper by Finite Element Method,” J. Intell. Mater. Syst. Struct. (2020).

[7] Amjadian, M. and Agrawal, A. K., “A passive electromagnetic eddy current friction damper (PEMECFD): Theoretical and analytical modeling,” Struct. Control Heal. Monit. **24**(10), e1978 (2017).

[8] Amjadian, M. and Agrawal, A. K., “Modeling, design, and testing of a proof-of-concept prototype damper with friction and eddy current damping effects,” J. Sound Vib. **413**, 225–249 (2018).

[9] El-hami, M., Glynne-Jones, P., White, N. M., Hill, M., Beeby, S., James, E., Brown, A. D. and Ross, J. N., “Design and fabrication of a new vibration-based electromechanical power generator,” Sensors Actuators, A Phys. **92**(1–3), 335–342 (2001).

[10] Beeby, S. P., Torah, R. N., Tudor, M. J., Glynne-Jones, P., O’Donnell, T., Saha, C. R. and Roy, S., “A micro electromagnetic generator for vibration energy harvesting,” J. Micromechanics Microengineering **17**(7), 1257–1265 (2007).

[11] Zeng, P. and Khaligh, A., “A permanent-magnet linear motion driven kinetic energy harvester,” IEEE Trans. Ind. Electron. **60**(12), 5737–5746 (2013).

[12] Elvin, N. G. and Elvin, A. A., “An experimentally validated electromagnetic energy harvester,” J. Sound Vib.

330(10), 2314–2324, Academic Press (2011).
[13] Kwon, S.-D., Park, J. and Law, K., "Electromagnetic energy harvester with repulsively stacked multilayer magnets for low frequency vibrations," Smart Mater. Struct. **22**(5), 055007 (2013).
[14] Halim, M. A., Cho, H. and Park, J. Y., "Design and experiment of a human-limb driven, frequency up-converted electromagnetic energy harvester," Energy Convers. Manag. **106**, 393–404 (2015).
[15] Salauddin, M., Halim, M. A. and Park, J. Y., "A magnetic-spring-based, low-frequency-vibration energy harvester comprising a dual Halbach array," Smart Mater. Struct. **25**(9), 095017 (2016).
[16] Liu, X., Qiu, J., Chen, H., Xu, X., Wen, Y. and Li, P., "Design and Optimization of an Electromagnetic Vibration Energy Harvester Using Dual Halbach Arrays," IEEE Trans. Magn. **51**(11) (2015).
[17] Peigney, M. and Siegert, D., "Low-Frequency Electromagnetic Energy Harvesting from Highway Bridge Vibrations," J. Bridg. Eng. **25**(8), 04020056 (2020).
[18] Soliman, M. S. M., Abdel-Rahman, E. M., El-Saadany, E. F. and Mansour, R. R., "A wideband vibration-based energy harvester," J. Micromechanics Microengineering **18**(11) (2008).
[19] Mikoshiba, K., Manimala, J. M. and Sun, C., "Energy harvesting using an array of multifunctional resonators," J. Intell. Mater. Syst. Struct. **24**(2), 168–179 (2013).
[20] Foisal, A. R. M., Hong, C. and Chung, G. S., "Multi-frequency electromagnetic energy harvester using a magnetic spring cantilever," Sensors Actuators, A Phys. **182**, 106–113 (2012).
[21] Arroyo, E., Badel, A., Formosa, F., Wu, Y. and Qiu, J., "Comparison of electromagnetic and piezoelectric vibration energy harvesters: Model and experiments," Sensors Actuators, A Phys. **183**, 148–156 (2012).
[22] Sazonov, E., Pillay, P., Li, H. and Curry, D., "Self-Powered Sensors for Monitoring of Highway Bridges," IEEE Sens. J. **9**(11), 1422–1429 (2009).
[23] Fu, Y., Ouyang, H. and Davis, R. B., "Triboelectric energy harvesting from the vibro-impact of three cantilevered beams," Mech. Syst. Signal Process. **121**, 509–531 (2019).
[24] Humar, J., [Dynamics of Structures, 3rd ed.], CRC Press (2012).
[25] Erturk, A. and Inman, D. J., "On Mechanical Modeling of Cantilevered Piezoelectric Vibration Energy Harvesters," J. Intell. Mater. Syst. Struct. **19**(11), 1311–1325 (2008).
[26] Furlani, E. P., [Permanent magnet and electromechanical devices], Academic Press (2001).
[27] Amjadian, M. and Agrawal, A. K., "A passive electromagnetic eddy current friction damper (PEMECFD): Theoretical and analytical modelling," Struct. Control Heal. Monit. (2017).
[28] Amjadian, M. and Agrawal, A. K., "Analytical modeling of a simple passive electromagnetic eddy current friction damper," SPIE Smart Struct. Mater. + Nondestruct. Eval. Heal. Monit. **9799**, G. Park, Ed., 1–14, International Society for Optics and Photonics (2016).
[29] Amjadian, M. and Agrawal, A. K., "Seismic response control of multi-story base-isolated buildings using a smart electromagnetic friction damper with smooth hysteretic behavior," Mech. Syst. Signal Process. **130**, 409–432 (2019).
[30] Amjadian, M. and Agrawal, A. K., "Vibration control using a variable coil-based friction damper," Proc. SPIE - Int. Soc. Opt. Eng. **10164** (2017).
[31] Amjadian, M. and Agrawal, A. K., "Feasibility study of using a semiactive electromagnetic friction damper for seismic response control of horizontally curved bridges," Struct. Control Heal. Monit., e2333 (2019).
[32] Zhu, S., Shen, W. ai and Xu, Y. lin., "Linear electromagnetic devices for vibration damping and energy harvesting: Modeling and testing," Eng. Struct. **34**, 198–212 (2012).
[33] Zuo, L. and Cui, W., "Dual-functional energy-harvesting and vibration control: Electromagnetic resonant shunt series tuned mass dampers," J. Vib. Acoust. Trans. ASME **135**(5) (2013).
[34] Shen, W., Zhu, S., Xu, Y.-L. and Zhu, H., "Energy regenerative tuned mass dampers in high-rise buildings," Struct. Control Heal. Monit. **25**(2), e2072 (2018).
[35] Cannarella, J., Selvaggi, J., Salon, S., Tichy, J. and Borca-Tasciuc, D. A., "Coupling factor between the magnetic and mechanical energy domains in electromagnetic power harvesting applications," IEEE Trans. Magn. **47**(8), 2076–2080 (2011).
[36] Mösch, M. and Fischerauer, G., "A Comparison of Methods to Measure the Coupling Coefficient of Electromagnetic Vibration Energy Harvesters," Micromachines **10**(12), 826 (2019).
[37] Erturk, A. and Inman, D. J., [Piezoelectric Energy Harvesting], John Wiley & Sons, Ltd, Chichester, UK (2011).
[38] "Simulink 9.0.", (2017).
[39] COMSOL v.5.4., "Multiphysics® Modeling Software v.5.4" (2018).
[40] Jia, Y., "Review of nonlinear vibration energy harvesting: Duffing, bistability, parametric, stochastic and

others," J. Intell. Mater. Syst. Struct. **31**(7), 921–944 (2020).